

**A TRACE ELEMENT INVESTIGATION INTO THE PETROGENETIC RELATIONSHIPS OF DIFFERENT IGNEOUS LITHOLOGIES WITHIN MARTIAN METEORITE NWA 7034.** A. R. Santos<sup>1</sup>, C. B. Agee<sup>1</sup>, C. K. Shearer<sup>1</sup>, P. V. Burger<sup>1</sup>, F. M. McCubbin<sup>1</sup>, <sup>1</sup>Institute of Meteoritics, 1 University of New Mexico, MSC03-2050, Albuquerque, NM 87131 (asantos5@unm.edu).

**Introduction:** Previous studies of the martian meteorite NWA 7034 and its pairings NWA 7533 and NWA 7475 indicate these meteorites are some of the most incompatible element enriched samples yet obtained from Mars [1, 2]. As these meteorites are breccias, in situ studies are required to determine which domains specifically carry the enriched signature. The geochemistry of the different meteorite domains will also aid in deciphering the origin and relationships of these materials. This investigation is the first portion of a study that will use pyroxene, plagioclase (the two major minerals within NWA 7034), and phosphates to assess the relationships and petrogenesis of the different domains of this meteorite (following [3]).

Several previous studies [e.g. 1, 4, 5] have reported different types of clasts within NWA 7034, which are suspended in a fine grained matrix that also contains large, isolated mineral fragments. We place the mineral chemical data within the context of the classification scheme of [4], which identified basaltic, basaltic andesite, and trachyandesite clasts within this meteorite. Pyroxenes from these three clast types, as well as isolated fragments surrounded by matrix, have similar major element contents (discussed in [6]), but have different textures, indicating different cooling histories, and the different clast types also contain different mineral assemblages. Using an integration of major and trace element analyses of the pyroxene and associated mineral phases, we deciphered the petrogenetic relationships among these lithologies.

**Methods:** Pyroxene grains were classified based on criteria discussed in [6]. Major element contents were determined using the JEOL 8200 Superprobe with Probe for EPMA software located at UNM. Abundances of eight REEs were determined using a Cameca ims 4F SIMS also located at UNM. SIMS data was collected using a 10 kV accelerating voltage, 30 nA beam current, voltage offset of -75 V, and a 30  $\mu$ m spot size. Apertures were used to sample smaller grains. An in house clinopyroxene standard was used for calibration and trace element intensities were normalized to SiO<sub>2</sub> contents measured using EPMA.

**Results:** The major element compositions of pyroxene analyzed for REEs in the study are partially represented in the pyroxene quadrilateral shown in Figure 1. These pyroxenes are from four igneous clasts and eight isolated fragments. The igneous clasts in-

cluded two basaltic clasts, one basaltic andesite clast, and one trachyandesite clast (clast types discussed in [4] with details on pyroxene major element chemistries presented in [6]). REE patterns for these selected pyroxenes are presented in Figure 2. Figure 2A contains the REE patterns for pyroxene grains with Wo<5 mol%. These grains have a slight LREE depletion and HREE enrichment, with the exception of three grains analyzed in a single basaltic clast that have a flat REE pattern. Eu anomalies are positive for some of these grains. Figure 2B contains the REE patterns for pyroxene grains with Wo between 6 and 50 mol%. In contrast to the low Wo group, these grains have a depleted LREE pattern and are enriched in HREEs. The different shapes of the REE patterns between the low and high Wo pyroxenes are a reflection of crystal chemical constraints on REE partitioning into pyroxene [7, 8]. For example, the Yb/Ce ratio for the low Wo pyroxenes is greater than that for the high Wo pyroxenes because augitic pyroxene has a larger M2 and can better accommodate the large LREEs. Exceptions to this are the three grains measured from a single basaltic clast shown in Figure 2A that have flat REE patterns. The patterns from different grains are parallel but vary in depth of Eu anomaly. The basaltic andesite clast contains REE abundances that are near the average for the matrix grains.

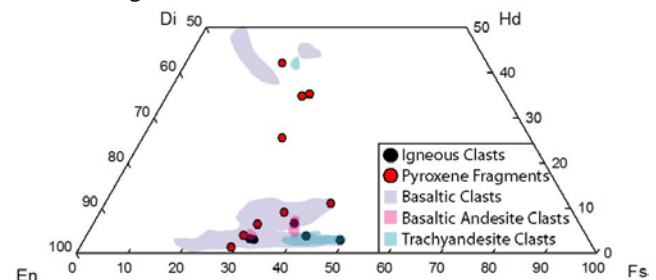


Figure 1: Ternary pyroxene average compositions for grains analyzed for REEs. Pyroxene trends for the different clast types shown in shaded regions.

The REE content of pyroxene in a bulk rock sample from [9] is also shown for comparison. The bulk rock pyroxene pattern is parallel to that of the 6-50 mol% Wo group, falling at abundances matching those found in the basaltic andesite clast. The Wo<5% group has a smaller LREE depletion than the bulk rock pyroxene pattern. Major element chemistry of the bulk rock sample indicates at Wo content ~5%, which is at the border of the two pyroxene groups defined in this study [9].

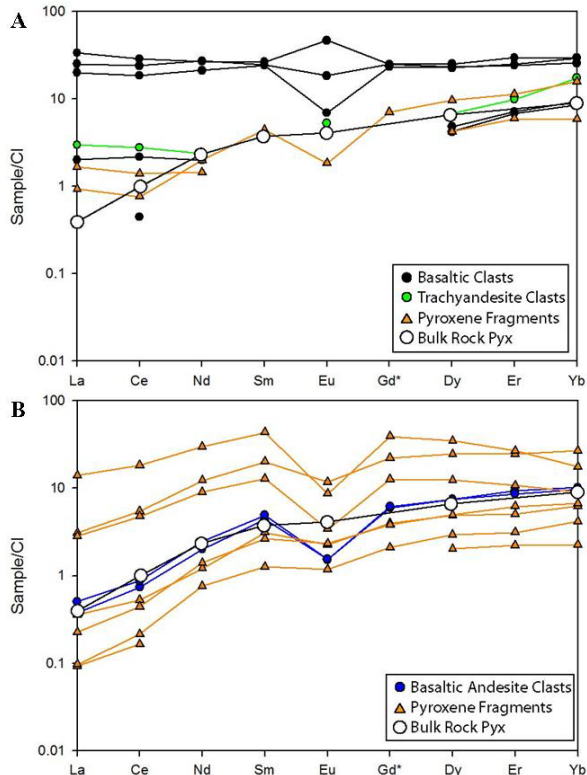


Figure 2: CI normalized REE patterns for pyroxene grains in different domains of NWA 7034 (CI abundances from [10]). A: Pyroxenes with  $W_o < 5\%$ . B: Pyroxenes with  $W_o$  between 6% and 50%. Gd is estimated by averaging Sm and Dy. Bulk rock pyroxene is from [9].

**Discussion:** The parallel REE patterns of the high  $W_o$  content group suggest derivation from the same parent magma. Comparison of the low  $W_o$  content group patterns is complicated by incomplete REE patterns due to low abundances in these grains. It appears most of the patterns in this group are parallel, with the exception of three patterns derived from a single basaltic clast (three highest La contents). These patterns are flat with one showing a positive Eu anomaly. Positive or near positive Eu anomalies are displayed in other pyroxene REE patterns from this meteorite, and have also been observed in apatite from an additional clast type [11]. These could be indicating a difference in oxidation state during crystallization for some of the materials, or could be due to ion beam overlap with surrounding plagioclase. The flat REE pattern displayed in the basaltic clast pyroxenes is likely not due to beam overlap, as two of the flat patterns show a negative Eu anomaly.

Figure 3 shows pyroxene REE data from [12] for three other martian basaltic shergottites. The NWA 7034 pyroxenes contain higher REE abundances than those in Los Angeles, the most enriched shergottite. This suggests NWA 7034 contains materials derived

from the most REE enriched martian magma sampled to date.

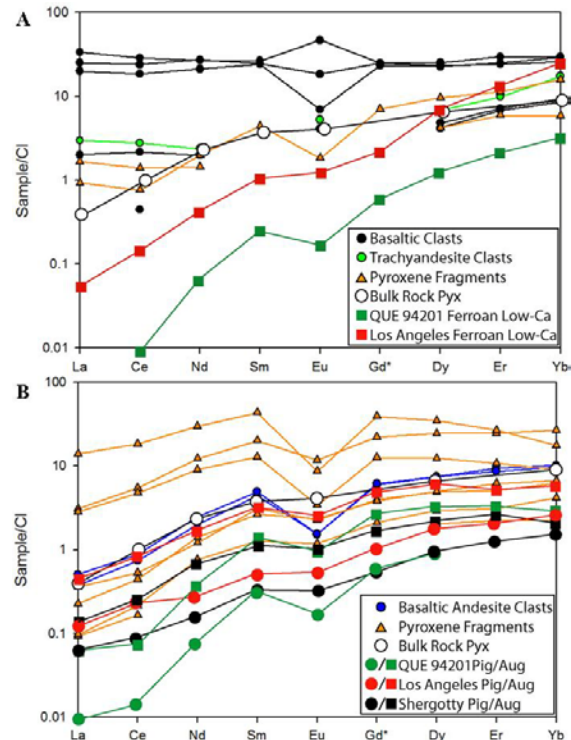


Figure 3: Comparison of CI normalized REE data from Fig. 2 with data from pyroxenes in QUE 94201, Shergotty, and Los Angeles obtained by [12]. A: Pyroxenes with  $W_o < 5\%$ . B: Pyroxenes with  $W_o$  between 6% and 50%.

Major element compositions of pyroxenes from different lithologies within NWA 7034 are overlapping, indicating there is no unique composition that can identify specific lithologies. However, the current data does show some trends that could help distinguish the different lithologies. For example, the basaltic andesite clasts do not contain pyroxene with  $W_o > 10$  mol%. Likewise, pyroxene REEs do not appear to be unique identifiers with respect to different lithologies. Continuing data collection on pyroxenes from these lithologies will reveal trends that, when paired with major element chemistries, may be able to be used as unique lithology identifiers.

**References:** [1] Agee C.B. et al. (2013) *Science*, 339, 780-785. [2] Humayun M. et al. (2013) *Nature*, 503, 513-516. [3] Papike J. J. et al. (1996) *GCA*, 60, 3967-3978. [4] Santos A.R. et al. (2013) *Meteoritics & Planetary Sci.*, 48, A306. [5] Hewins R. H. et al. (2013) *Meteoritics & Planet. Sci.*, 48, A160. [6] Santos et al. this meeting [7] Papike J. J. et al. (1988) *LPSC XIX*, Abstract #901. [8] Shearer C. K. et al. (1988) *LPSC XIX*, Abstract #1073. [9] Nyquist L. E. et al. (2013) *Meteoritics & Planet. Sci.*, 48, A270. [10] Anders E. and Grevesse N. (1989) *GCA*, 53, 197-214. [11] Santos A. R. et al. (2013) *LPSC XLIV*, Abstract #2601. [12] Wadhwa M. et al. (2001) *LPSC XXXII*, Abstract #1106.